Frequency-Domain Simulation and Time-Domain Measurements of a GaN Amplifier driven by M-QAM modulated carrier generator

C Hallepee, D Passerierieux, G Neveux, D Barataud

Frequency-Domain Simulation and Time-Domain Measurements of a GaN Amplifier driven by M-QAM modulated carrier generator.

C. Hallepee, D. Passererieux, G. Neveux, D. Barataud

XLIM Laboratory, UMR CNRS n°7252, University of Limoges, France
{clement.hallepee, damien.passerieux, guillaume.neveux, denis.barataud}@xlim.fr

***Abstract* — A new method is applied to perform, by Harmonic Balance (HB) techniques, the simulation of a GaN Doherty Power Amplifier (DPA) driven by carrier Random-Modulated (RM) signals. This article presents an example (16-QAM) of a driving random modulated voltage generated in the frequency-domain and the software-defined demodulation of the output signal of the DPA implemented with optimal matched filters to respect the Nyquist criteria. It allows the extraction of all the linearity and power metrics performances at design circuit level in the time and frequency-domains. For instance, dynamic power and linearity (Adjacent Channel Power Ratio (ACPR), Error Vector Magnitude (EVM)) performances are calculated. The simulated dynamic results are shown and compared to the measured results obtained on a specific THA-based time-domain calibrated test-bench developed in our laboratory. The Quasi-MMIC DPA under test is driven by a 3.5 GHz carrier frequency modulated with a 16-QAM signal for two different symbol rates.**

***Keywords* — circuit simulation; demodulation; frequency-domain analysis; harmonic balance; linearity; load modulated power amplifiers; modulation; non-linear circuits; pseudo-random generation**

I. Introduction

The main challenges that RF front-ends will have to face in the future are the following ones: the ecological footprint, the ability to transmit a large quantity of information at very high speed and the ability to perform this transmission with low distortion. In these front-ends, the RF power amplifier (PA) is one of the most important key part. The optimal circuit-level design of this power amplifier requires a fine-trade-off between the power added efficiency (PAE), the output power (P_{out}), the linearity, the RF Bandwidth (BW_{RF}) and the Modulation Bandwidth (BW_{mod}). In the first step of the power amplifier design, the simulations are generally carried out using continuous wave harmonic balance (CW-HB): a generator delivers a pure RF carrier frequency (f_{car}). Frequency and power are swept in order to perform the joint optimization of PAE, P_{out}, BW_{RF}, and quasi-static linearity. This optimization is generally performed through the investigation and visualization of the simulated plots of Power Gain (G_p), P_{out}, PAE, AM/AM and phase characteristics (AM/PM). However, CW HB simulations do not enable knowing the electrical behavior of the power amplifier in the presence of modulated signals as they are in real life. The power characteristics of the PA driven by modulated signals are measured a posteriori. For instance, for a known modulation format, ACPR or EVM are usually measured characteristics.

To apply the Pseudo-Random Modulation by Harmonic Balance techniques (PRM-HB) described here, the frequency grid is determined using two fundamental frequencies: the first one is associated to the carrier frequency (f_{car}) and the second one is related to the random modulation sequence ($f_{modframe}$) [1]. The value of $f_{modframe}$ is calculated as the inverse of the modulation frame time length (t_{stop}-t_{start}). For an M-QAM modulation with M complex levels, the frame length corresponds to an integer number of M. This configuration leads to a periodization of the modulation frame. The circuit is then considered as an almost-periodic circuit with two frequencies f_{car} and $f_{modframe}$ not harmonically related.

The paper presents the dynamic results obtained with the proposed PRM-HB simulation method applied to the DPA designed at UMS [1] driven by 16-QAM PRM signals. Thanks to a full spectrum time-domain measurement system (as opposed to a bandpass spectrum) the experimental results are finally compared with the outcomes obtained from the PRM-HB simulations.

II. 16 QAM PRM-HB Simulation of a 20W/S-Band Asymmetric DPA

A. Description of the DPA.

The designed DPA [2], shown in Fig. 1, combines GaN power bars and input/output matching circuits realized on passive GaAs MMICs technology specifically developed for high power density functions. Transistors of the power bars are based on 0.25µm AlGaN/GaN technology (GH25-10) from UMS foundry [3]. The design needs to consider the constraints of the quasi-MMIC technology thanks to a full 3D EM simulation of the interconnection network into the QFN environment.

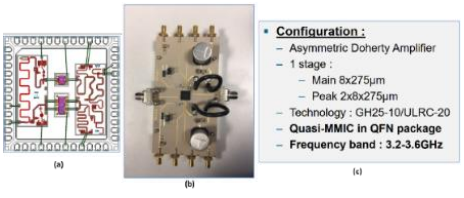

Fig. 1. Layout (a), Demonstration board (b) and Key Characteristics (c) of the realized asymmetric packaged Quasi-MMIC SI-DPA [2].

B. ADS Schematic and PRM-HB Simulation results of the 20W/S-Band Quasi-MMIC asymmetric DPA

A modulated EMF, $e_{modK}(t)$, with a carrier at a f_{car} frequency, and a periodic modulating signal with a fundamental frequency $f_{modframe}$ and K harmonics, can be written as:

$$e_{modK}(t) = \sum_{k=-K}^{k=K} A_k \cos\left(2\pi\left(f_{car} + k f_{modframe}\right)t + \varphi_k\right) \quad (1)$$

Because the simulated DPA is nonlinear, it generates harmonics of the carrier frequency and of the periodic modulating signal, leading to intermodulation frequencies. For the simulation, the harmonic frequencies are truncated respectively to N and K'.

Finally, all voltages or currents of the PRM-HB schematic, shown in Fig 2, can be written with the following generic waveform (x is replaced with "v_{mod}" or "v_{rec}" for voltages and "i_{mod}" or "i_{rec}"for currents):

$$x_{N,K'}(t) = \Re\left\{\left[\sum_{k=1}^{k=K'}\left(A_{k,0}e^{j\varphi_{k,0}}\right)e^{j2\pi k f_{modframe}t}\right]\right\} + \Re\left\{\sum_{n=1}^{n=N}\left[\sum_{k=-K'}^{k=K'}\left(A_{k,n}e^{j\varphi_{k,n}}\right)e^{j2\pi k f_{modframe}t}\right]e^{j2\pi n f_{car}t}\right\}$$

$$\text{with } nf_{car} + kf_{modframe} \geq 0 \quad (2)$$

From the simulated $\tilde{V}_{mod}(f)$ and $\tilde{V}_{rec}(f)$ voltages at the input and output of the DPA, respectively, the demodulated, matched-filtered and time-domain-corrected complex envelopes at f_{car}, $\tilde{v}_{mod\_RC\_corr}(t)$, $\tilde{v}_{rec\_RC\_corr}(t)$, $\tilde{\imath}_{mod\_RC\_corr}(t), \tilde{\imath}_{rec\_RC\_corr}(t)$ are calculated as described and defined in [4].

The simulated envelope PRM-HB metrics of this DPA are then defined from the time-domain-corrected complex envelopes.

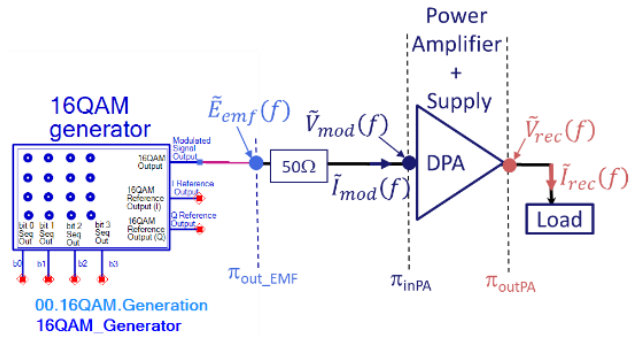

Fig. 2. Definitions of the frequency-domain variables for calculation of the modulated power performances.

The designed DPA is simulated with the configurations (with two different symbol rates) defined in Table 1.

Fig. 3 shows the average power performances calculated from the dynamic demodulated voltage envelopes $(\tilde{v}_{mod\_RC\_corr}(t), \tilde{v}_{rec\_RC\_corr}(t))$ for $S_{ymb}R_{ate1} = 1\text{MHz}$ and the sample at the average gain compression (maximum output power) for which one the time-domain and frequency-domain representations of the received characteristics/criteria of the DPA are extracted in Fig. 4.

Fig. 4 (a) presents the $|\tilde{V}_{rec}(f)|$ spectrum for A_{car} equal to 5.15V (maximum output power) and for $S_{ymb}R_{ate1} = 1\text{MHz}$. Fig 4 (b) shows the associated subsampled RF time domain $v_{rec\_subsamp}(t)$ zoomed between 2 µs and 8 µs.

Table 1. Parameters of the 16 QAM PRM-HB simulation of the DPA.

Parameter	Value with unit
Quiescent Main Voltage Drain	$V_{dsq_{main}} = 30V$
Quiescent Main Voltage Gate	$V_{gsq_{main}} = -3.78V$
Quiescent Peak Voltage Drain	$V_{dsq_{peak}} = 30V$
Quiescent Peak Voltage Gate	$V_{gsq_{peak}} = -5.5V$
CW Carrier Frequency	$f_{car} = 3.5$ GHz
Number of Symbols	$N_{symb} = 128$
Symbol Rate 1	$S_{ymb}R_{ate1} = 1\text{MHz}$
Symbol Rate 2	$S_{ymb}R_{ate2} = 10\text{MHz}$
Carrier Magnitude (V)	$0.15 \leq A_{car} \leq 5.15$ (Step: 0.1)
SRRC Roll Off	0.35
f_{car} HB Order (harmonics of the carrier frequency)	$N = 5$
$f_{modframe}$ HB Order (harmonics of the fundamental frequency of the periodic modulating signal)	$K' = 800$
Harmonic Order of the generated almost periodic modulated voltage signal $v_{modK}(t)$	$K = 86$

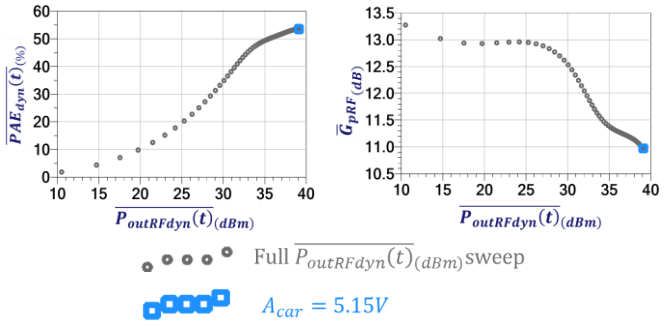

Fig. 3. Results of the PRM-HB simulation of the DPA driven by the modulated 16-QAM: $PAE_{(\%)}$ versus $\overline{P_{outRFdyn}(t)}_{(dBm)}$ (Left) and $PAE_{(\%)}$ versus $\overline{P_{outRFdyn}(t)}_{(dBm)}$ (Right) with indication of the selected samples for A_{car}=5.15V and for $S_{ymb}R_{ate1} = 1\text{MHz}$.

Fig. 4 (c) overlays $\tilde{v}_{ref}[p]$ with the corrected 16-QAM Vector Diagram $\tilde{v}_{rec\_RC\_samp\_corr}[p]$ and the EMF RC filtered Trajectory $\tilde{v}_{rec\_RC\_corr}(t)$ for $S_{ymb}R_{ate1} = 1\text{MHz}$.

Fig. 4 (d) overlays the dynamic drain efficiency $(DE_{dyn}(t)_{(\%)})$ versus dynamic output power $(P_{outRF}(t)_{(dBm)})$ curve extracted from the PRM-HB simulation with the CW drain efficiency $(DE_{(\%)})$ versus output power $(\bar{P}_{out}(f_0)_{(dBm)})$ obtained with the HB simulation. In Fig. 4 (d), the average point $(\overline{P_{outRF}(t)}_{(dBm)}, \overline{DE_{dyn}(t)}_{(\%)})$ is also indicated.

In Fig. 4 (d), the dynamic drain efficiency $DE_{dyn}(t) = f[P_{outRF}(t)]$ curve for $S_{ymb}R_{ate1} = 1\text{MHz}$ follows the equivalent CW curve with more dispersion. The peak dynamic output power almost reaches the peak value of the CW curve.

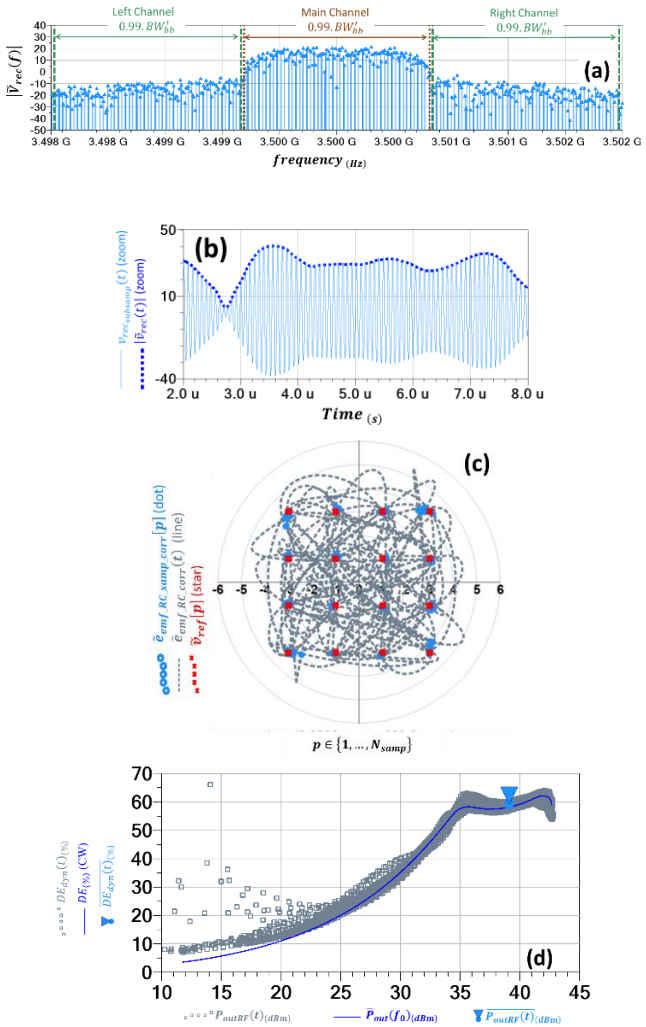

$\overline{P_{inRF}(t)} = 28.12$ dBm
$\overline{P_{outRF}(t)} = 39.10$ dBm
$\bar{G}_{pRF} = 10.97$ dB
$\overline{DE_{dyn}(t)} = 59.18$ %
$\overline{PAE_{dyn}(t)} = 54.54$ %
$EVM = 5.81$ %
$ACPR_{left} = -25.31$ dB
$ACPR_{right} = -24.82$ dB

Fig. 4. Main results of the PRM-HB simulation of the DPA driven by the modulated 16-QAM EMF for $A_{car} = 5.15V$ and for $S_{ymb}R_{ate1} = 10$MHz.

III. Time-Domain Set-up and Power Measurement Results of DPA Driven with Modulated Signals.

Fig. 5 describes the proposed 8-channel time-domain measurement system based on the use of track-and-hold amplifiers (THAs) [5]. The 8-channel measurement test bench contains two 20 dB wideband bidirectional couplers. The signal generated with the vector signal generator is linearly amplified using a broadband high gain amplifier before feeding the DPA. It also employs a large bandwidth [DC:1.6 GHz] digitizer to measure the fully calibrated coherent RF and LF voltage and current responses. 2 different channels of the 8-channel digitizers are also used to measure the raw LF output voltage and current of the DPA simultaneously with the envelopes of the RF voltages and currents. The RF calibration process performed for all the frequencies of the frequency grid (baseband, upper and lower sidebands around f_{car}) is based on three different steps: The first one is a classical SOLR [6] VNA calibration at all frequencies of interest. The second one is a power calibration based on the use of a power probe connected to the π_{inDPA} plane (Fig. 5) for the upper and lower sidebands around f_{car}.

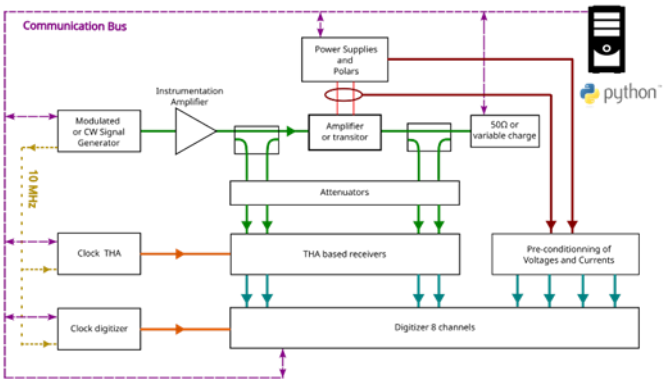

Fig. 5. 8-channel time-domain measurement system for power measurements of non-linear devices, driven by the CW signal and injected in the π_{inDPA} plane.

The last step is an absolute phase calibration based on a calibrated scope measurement standard for the upper and lower sidebands around f_{car}.

The six-channel measurement THA-based measurement set-up is then used to perform the measurement of the coherent RF and LF voltage and current responses of the DPA driven with the same 16-QAM 1MS/s and 10 MS/s modulated signals as the ones used in the simulation. The measured RF metrics of this HPA driven with a modulated signal are based on the measured power waves defined in the frequency-domain.

IV. Comparison Between 16-QAM PRM-HB Simulations and Time-Domain Measurements.

The comparison of the main power performances between simulation and measurements for the QAM 16 (1MS/s and 10MS/s) modulated signal are given in the following figures.

The measured and simulated CW and dynamic $\overline{PAE}$ (%) versus $\bar{P}_{out}(f_0)_{(dBm)}$ curves of the DPA driven with the CW signal @ 3.5 GHz and with the 16-QAM modulated signal at 1MS/s and 10 MS/s are compared in Fig. 6.

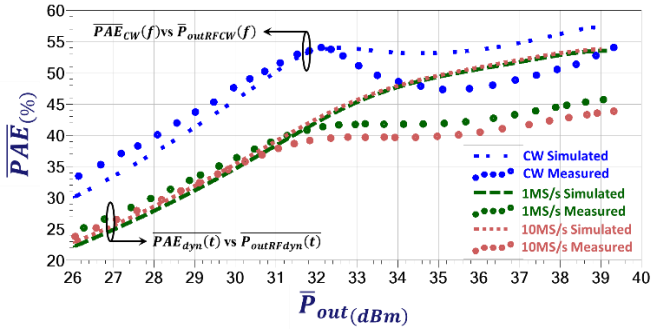

Fig. 6. Simulated/Measured CW and Dynamic $\overline{PAE}$ vs CW and Dynamic $\overline{P_{outRF}}$ (16-QAM modulated signal at 1MS/s and 10MS/s for dynamic curves).

Fig. 6 shows a light difference between the two modulation frequencies and the simulation is more optimistic that the measurements. The measured and simulated dynamic left

$ACPR$ versus $\overline{P_{outRFdyn}(t)}$ curves of the DPA driven with the 16-QAM modulated signal at 1MS/s and 10 MS/s are compared in Fig. 7.

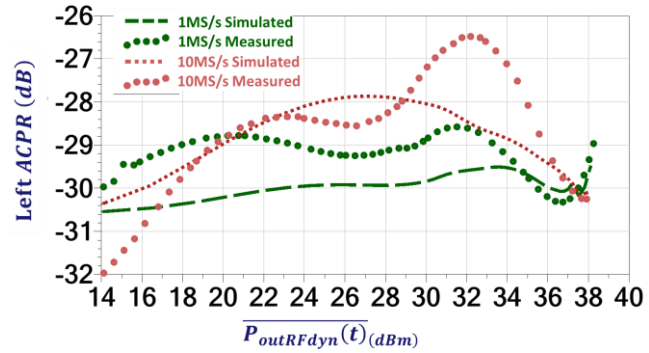

Fig. 7. Simulated/Measured Left $ACPR$ vs $\overline{P_{outRFdyn}(t)}$ of the DPA driven with the 16-QAM modulated signal at 1MS/s and 10MS/s.

The measured and simulated dynamic right $ACPR$ versus $\overline{P_{outRFdyn}(t)}$ curves of the DPA driven with the 16-QAM modulated signal at 1MS/s and 10 MS/s are compared in Fig. 8.

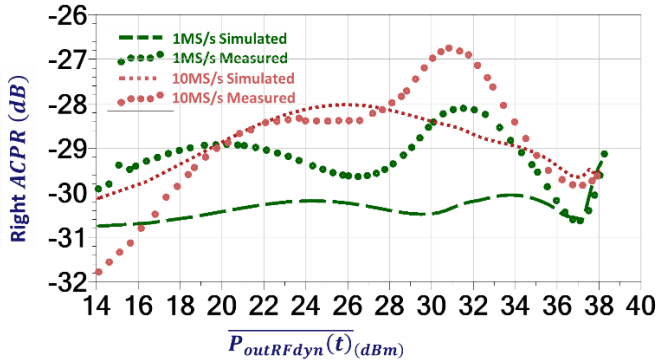

Fig. 8. Simulated and Measured Power performances of the DPA (Right $ACPR$ vs $\overline{P_{outRFdyn}(t)}$) driven with the 16-QAM modulated signal at 1MS/s and 10MS/s.

The measured and simulated dynamic EVM versus $\overline{P_{outRFdyn}(t)}$ curves of the DPA driven with the 16-QAM modulated signal at 1MS/s and 10 MS/s are compared in Fig. 9.

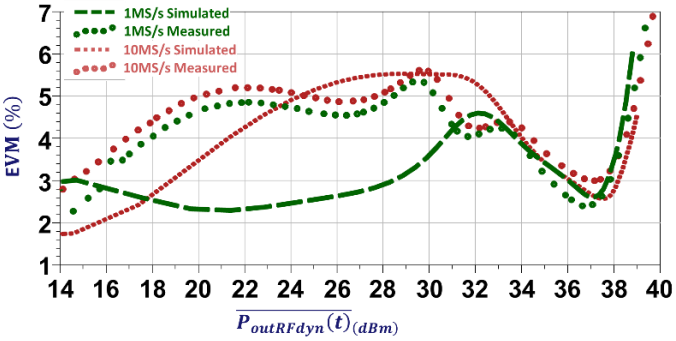

Fig. 9. Simulated and Measured Power performances of the DPA (EVM vs $\overline{P_{outRFdyn}(t)}$) driven with the 16-QAM modulated signal at 1MS/s and 10MS/s.

The figures 6 to 9 show a rather good agreement between measured and simulated results obtained with the 16-QAM modulated signal at 1MS/s and 10 MS/s validating the developed new PRM-HB simulation. The same simulations have to be performed also at the transistor level to also better understand the differences in the simulated ACPR and EVM for the two different frequencies. These simulations could also improve the understanding of parasitic effects as thermal and lags in the transistors and their effects when they are driven with different type of modulations with different modulation frequencies.

V. Conclusion

The new proposed method to perform Pseudo-Random-Harmonic Balance (PRM-HB) simulation, is applied to simulate a designed and fabricated 20W/S-Band Quasi-MMIC GaN asymmetric Doherty Power Amplifier. The simulated dynamic results are extracted from the PRM-HB simulation of the DPA driven by a 16-QAM signal at 1 MS/s and 10MS/s as example of modulated signals. The dynamic modulation criteria and power metrics (Adjacent-Channel Power Ratio (ACPR), Constellations and Vector Diagrams, Error Vector Magnitude (EVM)) simulated performances at design circuit level, in the frequency and time-domain, are calculated and compared to the ones obtained with a specific THA-based time-domain calibrated test-bench developed in our laboratory. These comparisons between measured and simulated results present rather good agreements, especially in the OBO region where the EVM presents local minimum values. To summarize, the PRM-HB is a real breakthrough as simulation tool and it also represents a very powerful and useful simulation tool in the frame of HPA feeding phased array antenna which leads to periodically modulated active reflection coefficients.

Acknowledgment

The authors are indebted to Professor J. Obregon for many discussions they shared with him. They also acknowledge M. Ayad and E. Richard, from UMS Foundry, who provided them with the GaN DPA and its associated schematics.

References

[1] Neveux G., Barataud D. “Simulation by Harmonic Balance Techniques of Non-Linear Circuits Driven by Random Modulated Signals.”. Submitted to 2024 19th European Microwave Integrated Circuit Conference, 2024.

[2] E. Richard, M. Ayad, M. Camiade, “Recent Development for Linear Amplification Based on GaN Technology” presented at the 12th European Microwave Integrated Conference (EUMIC) Conference of the EuMW, Recent Advancements in Wide-Band and Effcient GaN Power Amplifiers Workshop, WW-03, Nuremberg, Germany, Oct. 8-10, 2017.

[3] D. Floriot et al., "GH25-10: New qualified power GaN HEMT process from technology to product overview," 2014 9th European Microwave Integrated Circuit Conference, 2014, pp. 225-228, doi: 10.1109/EuMIC.2014.6997833.

[4] M. Ben-Sassi, G. Neveux and D. Barataud, "Ultra-Fast (13ns) Low Frequency/Microwave Transient Measurements, Application to GaN Transistors Characterization of Pulse to Pulse Stability," 2019 IEEE MTT-S International Microwave Symposium (IMS), Boston, MA, USA, 2019, pp. 1383-1386, doi: 10.1109/MWSYM.2019.8700727.

[5] Basu, S.; Hayden, L. An SOLR calibration for accurate measurement of orthogonal on-wafer DUTs. In Proceedings of the *1997 IEEE MTT-S International Microwave Symposium Digest*, Denver, CO, USA, 8–13 June 1997; Volume 3, pp. 1335–1338. https://doi.org/10.1109/MWSYM.1997.596575